

Supporting Information

High-Temperature Biferroicity in a Chiral 3D Hybrid Rare-Earth-Based Double Perovskite

Li-Ping Wang,^{1,2,#} Chang-Chun Fan,^{1,3,#} Zheng-Hui Hu,^{1,2} Hong-Fei Zhao,^{1,2} Jian-Rong Li,^{1,2,*} and Chao Shi^{1,2,*}

¹Jiangxi Province Key Laboratory of Functional Crystalline Materials Chemistry, Jiangxi University of Science and Technology, Ganzhou 341000, Jiangxi Province, P.R. China.

²Chaotic Matter Science Research Center, International Institute for Innovation, Jiangxi University of Science and Technology, Nanchang, Jiangxi, 330013, China.

³School of Materials Engineering, Jinling Institute of Technology, Nanjing 211169, P.R. China.

These authors contributed equally to this work.

*E-mail: jrli@fjirsm.ac.cn; 13064147687@163.com.

Supplementary Index

Experimental

General Measurements.

X-ray diffraction experiments.

Note

Note S1:

Supplemental Figures

Figure S1. PXRD patterns of **1** at room temperature.

Figure S2. The thermogravimetric (TG) curves of **1**.

Figure S3. DSC curves of **1** measured a cooling-heating cycle with different scanning rates.

Figure S4. Measurement of PXRD patterns of LTP, ITP, and HTP of **1**.

Figure S5. The SHG intensity of **1** is compared with that of the standard reference material KDP at room temperature.

Figure S6. Plot of SHG intensity obtained for switching experiment of **1** with $dT/dt = 30 \text{ K min}^{-1}$ between 330 and 440 K.

Figure S7. Switchable T - ϵ' curves of **1** measured at 500 Hz to 1 MHz.

Supplemental Tables

Table S1 The elemental analysis for **1**.

Table S2. Crystal data and refinement detail of **1** at 293 K, 390 K, and 428 K.

Table S3. The T_c based on organic, inorganic and other hybrid perovskite ferroelectrics and reported cases of this work.

Table S4. Selected bond lengths [\AA] and angles [$^\circ$] at 293 K, 390 K, and 428 K.

Experimental section

General Measurements.

Powder X-ray Diffraction (PXRD) patterns were collected on a Rigaku D/MAX 2000 PC diffractometer, utilizing Cu K α radiation ($\lambda = 0.15406$ nm) with a scanning range of 5°–50° and a rate of 5° min⁻¹. Thermogravimetric (TG) analysis was conducted under a nitrogen atmosphere using a NETZSCH STA2500 instrument at a heating rate of 10 K min⁻¹; approximately 10 mg of powdered compound 1 was loaded into an aluminum crucible for this purpose. Differential scanning calorimetry (DSC) experiments were performed in a nitrogen environment with a DSC 214 Polyma apparatus, maintaining a heating/cooling rate of 10 K min⁻¹. Dielectric measurements on compound 1 were executed using a Tonghui TH2828A impedance analyzer. The polycrystalline samples were pressed into pellets and sputtered with silver electrodes. The temperature-dependent complex dielectric permittivity ($\epsilon_r = \epsilon' - i\epsilon''$) was recorded across the frequency range of 500 Hz to 1000 kHz at temperatures between 260 K and 385 K. Ferroelastic domains were observed under an Olympus BX51TRF optical polarizing microscope, with temperature control maintained to within 0.2 K via an INSTRON HCC602 stage. Second harmonic generation (SHG) signals were measured using a pulsed Nd:YAG laser source (1064 nm, 5 ns pulses, 1.6 MW peak power, 10 Hz repetition rate). Variable-temperature ferroelectric P–E hysteresis loops were obtained on thin crystals (0.65 mm \times 0.10 mm) using a Radiant Precision Premier II system. Ferroelectric switching behavior was characterized via resonance-enhanced piezoresponse force microscopy (PFM) using an MFP-3D system (Asylum Research) with conductive Pt/Ir coated silicon probes (EFM-50, Nanoworld). Ultraviolet-visible (UV-Vis) absorption spectra were acquired on a Shimadzu UV-3600i Plus spectrometer (Japan) from 200 to 800 nm. Both steady-state emission spectra and time-resolved fluorescence lifetimes were determined using a FluoroLog 3-TCSPEC spectrofluorometer (Horiba Jobin Yvon Inc).

X-ray diffraction experiments.

Variable-temperature X-ray diffraction experiments were performed utilizing a Rigaku Synergy diffractometer equipped with Mo-K α radiation ($\lambda = 0.71073$ Å). The

processes of data collection, cell refinement, and data reduction were accomplished with the CrysAlisPro (v1.171.41.112a) XtaLAB Synergy-R online platform. Crystal structures were determined via direct methods and refined via full-matrix least-squares on F^2 with the OLEX2 software suite. Anisotropic refinement was applied to all non-hydrogen atoms, whereas hydrogen atom positions were set based on geometric calculations. Complete crystallographic details can be found in **Tables S1,S3**. Deposition of the crystal structure files (CIF) has been made with the Cambridge Crystal Data Center (**CCDC: 2445289–2445291**). Access to this material is provided free of charge by the Cambridge Crystallographic Data Centre.

Note

Note S1.

$$\begin{aligned} \Delta S_1 &= \int_{T_1}^{T_2} \frac{Q}{T} dT \approx \frac{\Delta H}{T_c} = \frac{6.757 \text{ J} \cdot \text{g}^{-1} \times 837.82 \text{ g} \cdot \text{mol}^{-1}}{370 \text{ K}} = \frac{11322}{370} \\ &= 15.3 \text{ J} \cdot \text{mol}^{-1} \cdot \text{K}^{-1} \end{aligned}$$

$$\Delta S_1 = R \ln N$$

$$N_1 = \exp\left(\frac{\Delta S}{R}\right) = \exp\left(\frac{15.3 \text{ J} \cdot \text{mol}^{-1} \cdot \text{K}^{-1}}{8.314 \text{ J} \cdot \text{mol}^{-1} \cdot \text{K}^{-1}}\right) = 6.300$$

$$\begin{aligned} \Delta S_2 &= \int_{T_1}^{T_2} \frac{Q}{T} dT \approx \frac{\Delta H}{T_c} = \frac{2.264 \text{ J} \cdot \text{g}^{-1} \times 837.82 \text{ g} \cdot \text{mol}^{-1}}{410.00 \text{ K}} = \frac{3793.6}{410} \\ &= 4.626 \text{ J} \cdot \text{mol}^{-1} \cdot \text{K}^{-1} \end{aligned}$$

$$\Delta S_1 = R \ln N$$

$$N_2 = \exp\left(\frac{\Delta S}{R}\right) = \exp\left(\frac{4.626 \text{ J} \cdot \text{mol}^{-1} \cdot \text{K}^{-1}}{8.314 \text{ J} \cdot \text{mol}^{-1} \cdot \text{K}^{-1}}\right) = 1.744$$

Supplemental Figures

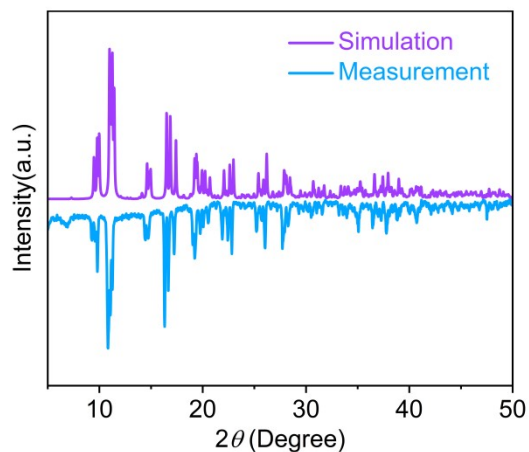


Figure S1. PXRD patterns of **1** were measured at room temperature.

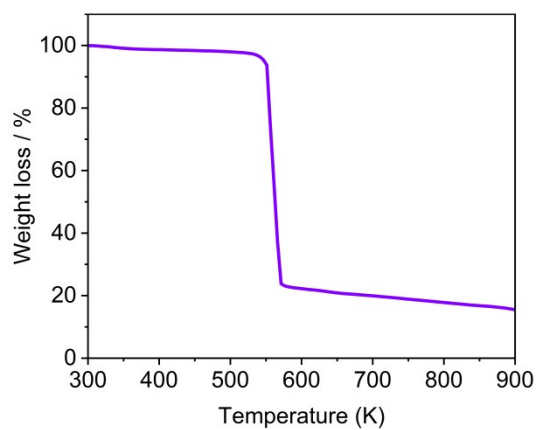


Figure S2. The thermogravimetric (TG) curves of **1** were recorded under a nitrogen atmosphere.

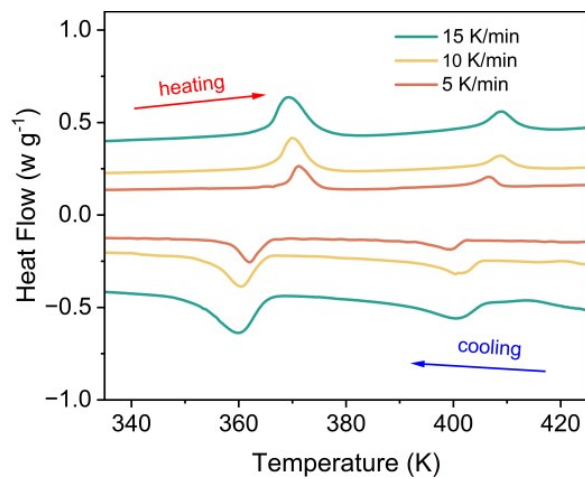


Figure S3. DSC curves of **1** measured a cooling-heating cycle with different scanning rates.

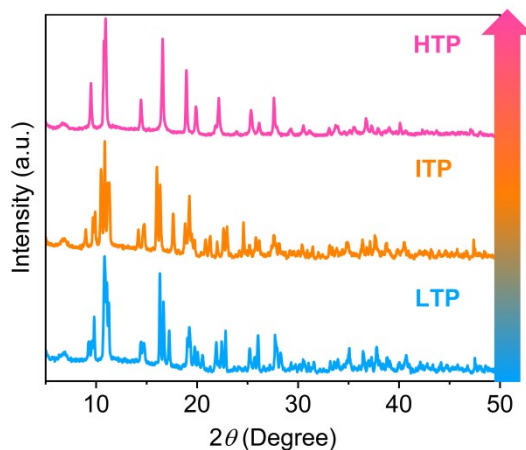


Figure S4. Measurement of PXRD patterns of LTP, ITP, and HTP of **1**.

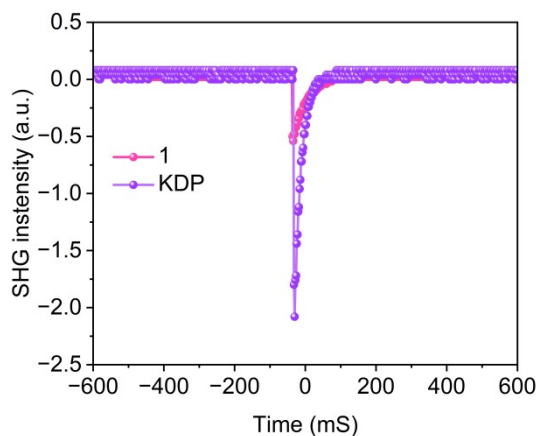


Figure S5. The SHG intensity of **1** is compared with that of the standard reference material KDP at room temperature.

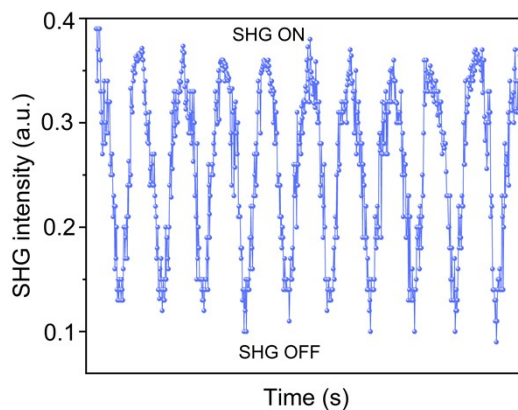


Figure S6. Plot of SHG intensity obtained for switching experiment of **1** with $dT/dt = 30 \text{ K min}^{-1}$ between 330 and 440 K.

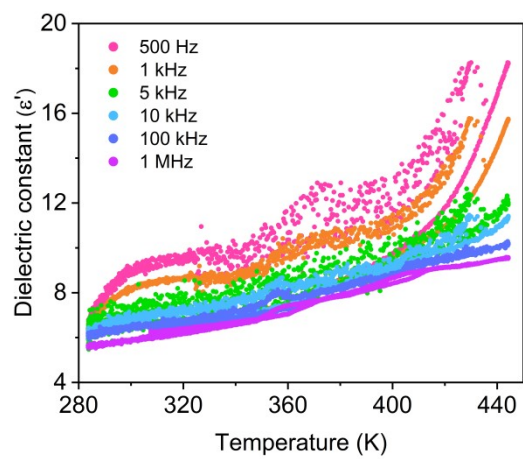


Figure. S7 Switchable T - ϵ' curves of **1** measured at 500 Hz to 1 MHz.

Supplemental Tables

Table S1 The elemental analysis for **1**.

(RM3HQ) ₄ K ₂ [Nd(NO ₃) ₆] ₂	Anal. (%)	Found (%)
C	22.88	22.84
H	3.84	3.86
N	13.34	13.38

The description of “The element analysis for **1**. Anal. (%) calc.: C 22.88, H 3.84, N 13.34. Found (%): C 22.84, H 3.86, N 13.38.”

Table S2. Crystal data and refinement detail of **1** at 293 K, 390 K, and 428 K.

<i>T</i> / K	293	390	428
Formula weight	837.82	809.77	779.56
Crystal system	monoclinic	monoclinic	monoclinic
Space group	<i>P</i> 2 ₁	<i>P</i> 2 ₁	<i>P</i> 6 ₃ 22
<i>a</i> / Å	10.1821(2)	9.97856(6)	10.6105(5)
<i>b</i> / Å	15.9260(3)	16.0494(6)	10.6105(5)
<i>c</i> / Å	18.6690(4)	10.7872(7)	16.2217(11)
<i>α</i> / °	90	90	90
<i>β</i> / °	91.366(2)	116.318(7)	90
<i>γ</i> / °	90	90	120
<i>V</i> / Å ³	3026.51(10)	1548.49(17)	1581.61(19)
<i>Z</i>	4	2	2
<i>λ</i> / Å	0.71073	0.71073	0.71073
<i>D</i> _{calc} / g·cm ⁻³	1.839	1.737	1.637
<i>μ</i> / mm ⁻¹	1.951	1.903	1.859
<i>F</i> (000)	1684	810	754
2 <i>θ</i> range / °	2.18–30.89	4.21–62.05	2.22–31.00
Reflns collected	32364	35254	12056
Independent reflns (<i>R</i> _{int})	14093 (0.0361)	8099 (0.0472)	2610 (0.0374)
No. of parameters	833	435	173
<i>R</i> ₁ ^[a] , <i>wR</i> ₂ ^[b] [<i>I</i> > 2σ(<i>I</i>)]	0.0362, 0.0859	0.0742, 0.1984	0.0540, 0.1299
<i>R</i> ₁ , <i>wR</i> ₂ [all data]	0.0424, 0.0891	0.1085, 0.2234	0.1069, 0.1615
GOF	1.024	0.963	0.956
Δ <i>ρ</i> ^[c] / e·Å ⁻³	0.96, -0.946	1.48, -0.87	0.39, -0.307
CCDC	2445289	2445290	2445291

^[a]*R*₁ = Σ||*F*_o|| - ||*F*_c|| / Σ||*F*_o||; ^[b]*wR*₂ = [Σ*w*(*F*_o² - *F*_c²)²] / Σ*w*(*F*_o²)²]^{1/2}; ^[c]maximum and minimum residual electron density.

Table S3. The *T*_c based on organic, inorganic and other hybrid perovskite ferroelectrics and reported cases of this work.

Compound	<i>T</i> _c / Ref.
----------	------------------------------

K		
Hybrid rare-earth double ferroelectrics		
$(RM3HQ)_2RbLa(NO_3)_6$	278	49
$(RM3HQ)_2RbPr(NO_3)_6$	280	41
$(RM3HQ)_2RbEu(NO_3)_6$	285	50
$(R3HQ)_4KCe(NO_3)_8$	323	39
$(R3HQ)_4KNd(NO_3)_8$	317	6
$(R3HQ)_4RbCe(NO_3)_8$	285	52
$(HQ)_4KEu(NO_3)_8$	291	53
$(S3HQ)_4EuRb(NO_3)_8$	94	54
$[(R)-CM3HQ]_2CsEu(NO_3)_6$	344	55
$[R-3-HDMP]_2RbSm(NO_3)_6$	251	56
$(RM3HQ)_4K_2[Nd(NO_3)_6]_2$	410	This work
Hybrid double ferroelectrics		
$(3\text{-Hydroxypyrrolidinium})_2RbBiBr_6$	432	51
$(R3HP)_2RbBiBr_6$	485	15
$[(CH_3)_3NOH]_2[KCo(CN)_6]$	416	10
$[(CH_3)_3NOH]_2[KFe(CN)_6]$	406	10
$(R-3P)_2KBiCl_6$	392	51
$(\text{chloropropylammonium})_4AgBiBr_8$	305	57
$(3,3\text{-difluorocyclobutanaminium})_4AgInBr_8$	230	58
$[CH_2CIN(CH_3)_3]_2NaRuCl_6$	320	59
$(FCH_2CH_2NH_3)_2[KFe(CN)_6]$	390	60

Table S4. Selected bond lengths [\AA] and angles [$^\circ$] at 293 K, 390 K, and 428 K.

293 K			
Nd(01)–O(005)	2.647(5)	O(005)–Nd(01)–O(006)	115.64(15)
Nd(01)–O(006)	2.697(5)	O(007)–Nd(01)–O(005)	177.23(17)
Nd(01)–O(007)	2.590(5)	O(007)–Nd(01)–O(006)	63.19(16)
Nd(01)–O(008)	2.570(5)	O(007)–Nd(01)–O(009)	69.89(16)
Nd(01)–O(009)	2.592(5)	O(007)–Nd(01)–O(00A)	116.40(16)
Nd(01)–O(00A)	2.605(4)	O(007)–Nd(01)–O(00C)	71.46(16)
Nd(01)–O(00C)	2.615(5)	O(007)–Nd(01)–O(00F)	131.89(16)
Nd(01)–O(00F)	2.638(4)	O(007)–Nd(01)–O(00G)	65.06(17)
Nd(01)–O(00G)	2.633(5)	O(007)–Nd(01)–O(00I)	113.27(16)
Nd(01)–O(00I)	2.603(5)	O(007)–Nd(01)–O(00U)	113.41(17)
Nd(01)–O(00P)	2.565(5)	O(008)–Nd(01)–O(005)	67.08(15)

Nd(01)–O(00U)	2.591(5)	O(008)–Nd(01)–O(006)	69.99(16)
Nd(02)–O(00E)	2.607(6)	O(008)–Nd(01)–O(007)	110.21(16)
Nd(02)–O(00J)	2.611(5)	O(008)–Nd(01)–O(009)	110.74(15)
Nd(02)–O(00Q)	2.614(5)	O(008)–Nd(01)–O(00A)	127.91(15)
Nd(02)–O(00R)	2.606(6)	O(008)–Nd(01)–O(00C)	175.07(16)
Nd(02)–O(00T)	2.582(6)	O(008)–Nd(01)–O(00F)	64.74(15)
Nd(02)–O(00V)	2.610(5)	O(008)–Nd(01)–O(00G)	49.27(16)
Nd(02)–O(012)	2.606(5)	O(008)–Nd(01)–O(00I)	69.80(15)
Nd(02)–O(014)	2.618(5)	O(008)–Nd(01)–O(00U)	114.47(16)
Nd(02)–O(016)	2.648(6)	O(009)–Nd(01)–O(005)	111.37(15)
Nd(02)–O(018)	2.588(5)	O(009)–Nd(01)–O(006)	47.83(15)
Nd(02)–O(01D)	2.648(5)	O(009)–Nd(01)–O(00A)	67.55(15)
Nd(02)–O(01E)	2.571(6)	(01E)–Nd(02)–O(01D)	175.97(18)
K(003)–O(00B)	2.925(5)	O(010)–K(003)–O(00B)	75.90(18)
K(003)–O(00L)	2.824(5)	N(00Z)–O(009)–Nd(01)	99.4(4)
K(003)–O(010)	2.780(6)	N(00Y)–O(00A)–Nd(01)	98.5(3)
K(003)–O(016)#1	3.024(6)	C(01C)–O(00B)–K(003)	116.4(4)
K(003)–O(018)#1	3.087(7)	N(00Y)–O(00C)–Nd(01)	97.0(3)
K(003)–O(01A)#2	2.830(6)	C(00X)–O(00D)–K(004)	119.6(4)
K(003)–O(01D)#1	3.026(6)	N(01L)–O(00E)–Nd(02)	98.2(5)
K(003)–O(01U)	2.820(6)	N(00W)–O(00F)–Nd(01)	97.6(3)
K(004)–O(006)#3	2.966(6)	O(010)–K(003)–O(00B)	75.90(18)
K(004)–O(007)#3	3.080(6)	N(00Z)–O(009)–Nd(01)	99.4(4)
K(004)–O(00D)	2.849(6)	N(00Y)–O(00A)–Nd(01)	98.5(3)
K(004)–O(00G)#3	3.018(6)	C(01C)–O(00B)–K(003)	116.4(4)
K(004)–O(00H)#2	2.992(6)	N(00Y)–O(00C)–Nd(01)	97.0(3)
K(004)–O(00O)	2.813(6)	C(00X)–O(00D)–K(004)	119.6(4)
K(004)–O(019)#4	2.919(6)	N(01L)–O(00E)–Nd(02)	98.2(5)
K(004)–O(026)	2.812(8)	N(00W)–O(00F)–Nd(01)	97.6(3)

Symmetry codes: #1: $-x, 1-y, 1-z$; #2: $1-x, 1-y, 2-z$; #3: $-0.5+x, 0.5-y, -0.5+z$; #4: $-0.5+x, 0.5-y, 0.5+z$; #5: $0.5+x, 0.5-y, 0.5+z$; #6: $0.5+x, 0.5-y, -0.5+z$.

390 K

Nd(1)–O(1)	2.609(16)	O(22)#1–Nd(1)–O(1)	113.0(6)
Nd(1)–O(4)	2.562(16)	O(22)#1–Nd(1)–O(6)	112.1(6)
Nd(1)–O(6)	2.571(18)	O(22)#1–Nd(1)–O(12)	111.1(6)
Nd(1)–O(12)	2.603(16)	O(22)#1–Nd(1)–O(16)#1	48.7(6)
Nd(1)–O(16)#1	2.633(15)	O(22)#1–Nd(1)–O(2)	66.9(6)
Nd(1)–O(22)#1	2.571(18)	O(22)#1–Nd(1)–O(19)	42.4(9)
Nd(1)–O(2)	2.604(15)	O(22)#1–Nd(1)–O(11)#2	178.9(7)
Nd(1)–O(9)	2.54(3)	O(2)–Nd(1)–O(1)	110.6(5)
Nd(1)–O(19)	2.61(3)	O(2)–Nd(1)–O(12)	67.2(5)
Nd(1)–O(5)	2.54(3)	O(2)–Nd(1)–O(16)#1	69.3(6)
Nd(1)–O(21)#2	2.56(2)	O(2)–Nd(1)–O(19)	81.3(9)
Nd(1)–O(11)#2	2.604(18)	O(2)–Nd(1)–O(11)#2	112.0(6)
K(1)–O(1)#3	3.15(2)	O(9)–Nd(1)–O(1)	89.8(9)
K(1)–O(8)#3	3.11(3)	O(9)–Nd(1)–O(12)	137.4(10)
K(1)–O(16)	2.960(17)	O(9)–Nd(1)–O(2)	147.7(10)
K(1)–O(18)	2.889(14)	O(9)–Nd(1)–O(19)	68.9(12)
K(1)–O(20)	2.861(16)	O(9)–Nd(1)–O(5)	70.4(11)
K(1)–O(3)#4	2.838(15)	O(9)–Nd(1)–O(11)#2	98.8(11)
K(1)–O(13)	2.92(2)	O(5)–Nd(1)–O(1)	145.9(10)
K(1)–H(13)	2.1498	O(5)–Nd(1)–O(12)	144.1(8)
K(1)–O(17)#3	3.16(4)	O(5)–Nd(1)–O(2)	100.1(9)
K(1)–O(23)	2.99(4)	O(5)–Nd(1)–O(19)	49.8(11)
O(1)–Nd(1)–O(12)	47.6(5)	O(5)–Nd(1)–O(11)#2	88.3(9)
O(1)–Nd(1)–O(16)#1	67.2(6)	O(21)#2–Nd(1)–O(1)	109.6(8)
O(1)–Nd(1)–O(19)	147.5(8)	O(22)#1–Nd(1)–O(1)	113.0(6)
O(1)–Nd(1)–O(11)#2	67.1(7)	O(22)#1–Nd(1)–O(6)	112.1(6)
O(4)–Nd(1)–O(1)	176.7(6)	O(22)#1–Nd(1)–O(12)	111.1(6)

O(4)–Nd(1)–O(6)	114.1(7)	O(22)#1–Nd(1)–O(16)#1	48.7(6)
O(4)–Nd(1)–O(12)	129.1(6)	O(22)#1–Nd(1)–O(2)	66.9(6)
O(4)–Nd(1)–O(16)#1	112.8(7)	O(22)#1–Nd(1)–O(19)	42.4(9)
O(4)–Nd(1)–O(22)#1	68.1(6)	O(22)#1–Nd(1)–O(11)#2	178.9(7)
O(4)–Nd(1)–O(2)	66.7(6)	O(2)–Nd(1)–O(1)	110.6(5)
O(4)–Nd(1)–O(11)#2	111.7(7)	O(2)–Nd(1)–O(12)	67.2(5)
O(6)–Nd(1)–O(1)	68.6(6)	O(2)–Nd(1)–O(16)#1	69.3(6)
O(6)–Nd(1)–O(12)	112.5(6)	O(2)–Nd(1)–O(19)	81.3(9)
O(6)–Nd(1)–O(16)#1	109.2(6)	O(2)–Nd(1)–O(11)#2	112.0(6)
O(6)–Nd(1)–O(2)	178.5(6)	O(9)–Nd(1)–O(1)	89.8(9)
O(6)–Nd(1)–O(11)#2	69.0(7)	O(9)–Nd(1)–O(12)	137.4(10)
O(12)–Nd(1)–O(16)#1	68.3(6)	O(9)–Nd(1)–O(2)	147.7(10)
O(12)–Nd(1)–O(19)	146.7(10)	O(9)–Nd(1)–O(19)	68.9(12)

Symmetry codes: #1: 2–x, 2–y, 1–z; #2: 2–x, +y, 1–z; #3: +x, 2–y, +z; #4: +x, 1–y, +z; #5: 1–x, +y, –z; #6: 1–x, 1–y, –z; #7: 1–x, +y, 1–z; #8: 1–x, –y, 1–z; #9: +x, –y, +z; #10: 1–x, 1–y, 1–z.

428 K

Nd(1)–O(15)#1	2.59(2)	O(15)#1–Nd(1)–O(15)#2	104.1(9)
Nd(1)–O(15)#2	2.59(2)	O(15)#1–Nd(1)–O(15)#3	104.1(9)
Nd(1)–O(15)#3	2.59(2)	O(15)#2–Nd(1)–O(15)#3	104.1(9)
Nd(1)–O(8)#1	2.592(16)	O(15)#1–Nd(1)–O(8)#1	34.1(8)
Nd(1)–O(8)#2	2.592(16)	O(15)#2–Nd(1)–O(8)#1	76.9(8)
Nd(1)–O(8)#3	2.592(16)	O(15)#3–Nd(1)–O(8)#1	131.0(9)
Nd(1)–O(1)#4	2.604(16)	O(15)#1–Nd(1)–O(8)#2	131.0(9)
Nd(1)–O(1)	2.604(16)	O(15)#2–Nd(1)–O(8)#2	34.1(8)
Nd(1)–O(1)#5	2.604(16)	O(15)#3–Nd(1)–O(8)#2	76.9(8)
Nd(1)–O(7)	2.60(2)	O(8)#1–Nd(1)–O(8)#2	110.2(5)
Nd(1)–O(7)#5	2.60(2)	O(15)#1–Nd(1)–O(8)#3	76.9(8)
Nd(1)–O(7)#4	2.60(2)	O(15)#2–Nd(1)–O(8)#3	131.0(9)
Nd(1)–O(2)#4	2.611(13)	O(15)#3–Nd(1)–O(8)#3	34.1(8)

Nd(1)–O(2)#5	2.611(13)	O(8)#1–Nd(1)–O(8)#3	110.2(5)
Nd(1)–O(2)	2.611(13)	O(8)#2–Nd(1)–O(8)#3	110.2(5)
Nd(1)–O(9)	2.61(3)	O(15)#1–Nd(1)–O(1)#4	135.1(8)
Nd(1)–O(9)#4	2.61(3)	O(15)#2–Nd(1)–O(1)#4	119.7(10)
Nd(1)–O(9)#5	2.61(3)	O(15)#3–Nd(1)–O(1)#4	76.3(9)
K(2)–O(4)#4	2.860(19)	O(8)#1–Nd(1)–O(1)#4	146.5(6)
K(2)–O(4)	2.860(19)	O(8)#2–Nd(1)–O(1)#4	93.4(6)
K(2)–O(4)#5	2.860(19)	O(8)#3–Nd(1)–O(1)#4	81.7(7)
K(2)–O(6)#4	2.99(8)	O(15)#1–Nd(1)–O(1)	119.7(10)
K(2)–O(6)#5	2.99(8)	O(15)#2–Nd(1)–O(1)	76.3(9)
K(2)–O(6)	2.99(8)	O(15)#3–Nd(1)–O(1)	135.1(8)
K(2)–O(2)	3.087(15)	O(8)#1–Nd(1)–O(1)	93.4(6)
K(2)–O(2)#4	3.087(16)	O(8)#2–Nd(1)–O(1)	81.7(7)
K(2)–O(2)#5	3.087(15)	O(8)#3–Nd(1)–O(1)	146.5(6)
K(2)–O(1)#4	3.106(18)	O(1)#4–Nd(1)–O(1)	66.0(7)
K(2)–O(1)#5	3.106(18)	O(15)#1–Nd(1)–O(1)#5	76.3(9)
K(2)–O(1)	3.106(18)	O(15)#2–Nd(1)–O(1)#5	135.1(8)
O(1)–N(2)	1.209(18)	O(15)#3–Nd(1)–O(1)#5	119.7(10)
O(2)–N(2)	1.209(17)	O(8)#1–Nd(1)–O(1)#5	81.7(7)
N(3)–O(15)	1.09(3)	O(8)#2–Nd(1)–O(1)#5	146.5(6)
N(3)–O(4)	1.20(3)	O(8)#3–Nd(1)–O(1)#5	93.4(6)
N(3)–O(8)	1.26(3)	O(1)#4–Nd(1)–O(1)#5	66.0(7)
O(8)–O(15)	1.52(3)	O(1)–Nd(1)–O(1)#5	66.0(7)
O(8)–Nd(1)#6	2.592(16)	O(15)#1–Nd(1)–O(7)	100.6(8)
O(15)–Nd(1)#6	2.59(2)	O(15)#2–Nd(1)–O(7)	49.6(7)

Symmetry codes: #1: 2–x, 2–y, 1–z; #2: 2–x, +y, 1–z; #3: +x, 2–y, +z; #4: +x, 1–y, +z; #5: 1–x, +y, –z; #6: 1–x, 1–y, –z; #7: 1–x, +y, 1–z; #8: 1–x, –y, 1–z; #9: +x, –y, +z; #10: 1–x, 1–y, 1–z.